JACS
JOURNAL OF THE AMERICAN CHEMICAL SOCIETY

ARTICLE

pubs.acs.org/JACS

# 1,9-Dialkoxyanthracene as a $^1O_2$-Sensitive Linker

Dumitru Arian, Larisa Kovbasyuk, and Andriy Mokhir*

Institute of Inorganic Chemistry, Ruprecht-Karls-University of Heidelberg, Im Neuenheimer Feld 270, 69120 Heidelberg, Germany

Supporting Information

**ABSTRACT:** We developed a $^1O_2$-sensitive linker based on a 9,10-dialkoxyanthracene structure. Its cleavage in the presence of $^1O_2$ is quick and high-yielding. A phosphoramidite containing this fragment was prepared and coupled to a variety of molecular fragments, including nucleosides, fluorescent dyes, and a cholesteryl derivative. On the basis of this building block we prepared a fluorogenic probe for monitoring $^1O_2$ in live mammalian cells and visible-light-activated "caged" oligodeoxyribonucleotides. In particular, the fluorogenic $^1O_2$ probe is a conjugate of 4,7,4′,7′-tetrachlorofluorescein and *N*,*N*,*N*′,*N*′-tetramethylrhodamine coupled to each other via the $^1O_2$-sensitive linker. Fluorescence of the dyes in this probe is quenched. In the presence of $^1O_2$, the linker is cleaved with formation of 9,10-anthraquinone and two strongly fluorescent dyes: 4,7,4′,7′-tetrachlorofluorescein and *N*,*N*,*N*′,*N*′-tetramethylrhodamine derivatives. We observed that the fluorescence of the probe correlates with the amount of $^1O_2$ present in solution. The red-light-activated "caged" oligodeoxyribonucleotides are stable duplexes, which consist of an unmodified strand and a blocker strand. The $^1O_2$-sensitive linker is introduced in the interior of the blocker strand. Upon exposure of the duplex to red light in the presence of $In^{3+}$(pyropheophorbide-*a*) chloride, the linker is cleaved with formation of the unstable duplex structure. This product decomposes spontaneously, releasing the unmodified strand, which can bind to the complementary target nucleic acid. This uncaging reaction is high-yielding. In contrast, previously reported visible-light-activated reagents are uncaged inefficiently due to competing reactions of sulfoxide and disulfide formation.

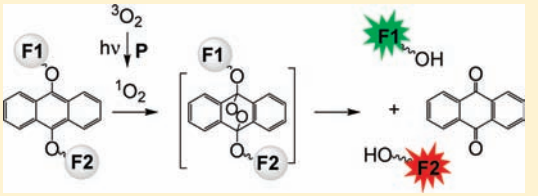


## INTRODUCTION

Photocleavable protecting groups are required to prepare "caged" biologically active molecules. Such molecules are inactive in the dark but become activated upon their exposure to light.[1] Light is an excellent trigger. In particular, it can be applied remotely, focused on the desired area, and switched on and off at will. Consequently, the activity of the "caged" reagents can be spatially and temporally controlled. A number of biologically active molecules have been produced in the "caged" form. For example, "caged" metal ion binders, ATP, cAMP, amino acids, neurotransmitters, steroids, sugars, lipids, nucleic acids, oligonucleotides, oligonucleotide analogues, siRNAs, peptides, and proteins are known.[1]

To cage nucleic acids or oligonucleotides, several protecting groups usually have to be placed on the corresponding biopolymer. Uncaging of the resulting reagents requires long irradiation time, and several equivalents of toxic side products (remainders of the corresponding protecting groups) are formed.[1b,e,g] Dmochowski and co-workers[2] have solved this problem by applying one photocleavable (PC) linker in place of several protecting groups. In the "caged" state of these improved reagents, the folded inactive oligonucleotide conformation is stable. When the PC linker is cleaved, the unfolded active form becomes more stable.

The majority of known PC protecting groups and linkers are cleaved by exposure to UV light.[1] Light of this type is strongly absorbed by cellular components and is damaging to cells.[3] Known undesirable photoreactions induced by UV light include dimerization of thymidine residues within genomic DNA and riboflavin-photosensitized generation of $^1O_2$. Moreover, UV light may directly affect gene expression.[4]

Stimulated by the earlier work of Breslow and co-workers[5] on photocleavable carriers for photosensitizers, we applied a visible- (>500 nm) light-controlled PC linker to prepare "caged" oligodeoxyribonucleotides (ODNs)[6] and phosphorothioate DNAs.[7] In contrast to UV light, >500 nm light is not toxic to mammalian cells. The PC linker contains a visible-light-absorbing photosensitizer (e.g., eosin) and a ~SCH=CHS~ fragment. Upon exposure to light, the photosensitizer generates singlet oxygen [$^1O_2$ or $O_2(^1\Delta_g)$],[8] which reacts further with the ~SCH=CHS~ to form a [2 + 2] cycloaddition product. The latter compound decomposes spontaneously with formation of two thioformate fragments (Scheme 1). The mechanism of this reaction has been thoroughly studied.[9]

One can envision that $^1O_2$-sensitive linkers such as ~SCH=CHS~ also can be applied to prepare fluorescent probes for detection of $^1O_2$ in live cells. Monitoring of $^1O_2$ is crucial for studying its role in cell transduction, gene regulation, and mediation of immune response as well as for estimation of the efficiency of photodynamic therapy (PDT)[8a] and for amplified detection of ribonucleic acids in live cells.[10]

Furthermore, $^1O_2$-sensitive linkers can find applications in nanotechnology. In particular, we have recently used ODN~SCH=CHS~biotin conjugates for chemical modification of predefined sites on the surface of DNA-Origami,[11] a nanostructure

**Received:** September 30, 2010
**Published:** February 23, 2011

  

**Scheme 1. Transformations of ~SCH=CHS~ Fragment in the Presence of $^1O_2$**[a] [6,7]

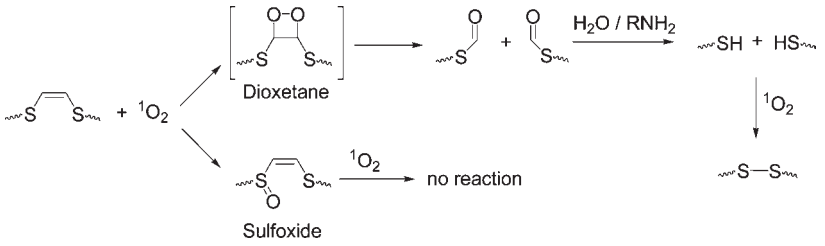


[a] $RNH_2$ is a natural amine, for example, from amino acids; $^1O_2$ is photogenerated in the presence of a photosensitizer, such as eosin or chlorin e6.

that is being actively explored in several laboratories as a scaffold for bottom-up manufacturing of electronic and optical nanodevices.[12]

Unfortunately, two undesired side reactions occur upon interaction of a ~SCH=CHS~ fragment with $^1O_2$. The first one is direct oxidation of the sulfur atom with formation of the corresponding sulfoxide [~S(O)CH=CHS~] (Scheme 1).[6,7] Since the C=C bond in the sulfoxide is not as electron-rich as that in ~SCH=CHS~, the follow-up cycloaddition reaction between $^1O_2$ and the sulfoxide does not take place. Thus, this side reaction lowers the yield of $^1O_2$-induced cleavage of the ~SCH=CHS~ linker. When the reaction is conducted at physiological conditions (water or/and amines are present in solution), acylated thiols initially formed as the result of spontaneous decomposition of the dioxetane are converted into thiols. The thiols are further oxidized by $^1O_2$, forming a disulfide group (Scheme 1). In the result of this second side reaction, one linker (~SCH=CHS~) is converted to another one (~S−S~) rather than cleaved.[6,7]

Herein we report on an improved $^1O_2$-sensitive linker: a 9,10-dialkoxyanthracene derivative. It is cleaved quickly and with high yield in the presence of $^1O_2$ both in vitro and in cells. On the basis of this fragment, we developed a fluorogenic probe for detection of $^1O_2$ in live mammalian cells and prepared improved "caged" ODNs, whose ability to hybridize to nucleic acids is controlled by nontoxic red light.

## RESULTS AND DISCUSSION

**Concept and Preliminary Experiments.** Known anthracene-based $^1O_2$ traps contain hydrogen or carbon substituents at positions 9 and 10 of the anthracene moiety.[13] These compounds react with $^1O_2$ via the highly favorable [4 + 2] cycloaddition mechanism, forming stable endoperoxides. We envisioned that 9,10-dialkoxy-substituted anthracenes (e.g., compound **1** in Scheme 2) would retain the ability to bind $^1O_2$ quickly and efficiently. In contrast, the endoperoxide product (**1**-$O_2$) formed in this reaction would spontaneously decompose in the follow-up proton-catalyzed reaction with formation of products **2**, **3**, and **4** (Scheme 2). To test this hypothesis, we first studied the reactivity of commercially available 9,10-dimethoxyanthracene **5** toward $^1O_2$. $^1O_2$ was generated by exposure of eosin (**P1**) or $In^{3+}$-(pyropheophorbide-*a*) chloride (**P2**)[14] to green or red light, respectively (Scheme 2). We were pleased to observe that compound **5** was converted to 9,10-anthraquinone derivative **4** in the presence of $^1O_2$ at pH 7.

**9,10-Di(3-hydroxypropoxy)anthracene as a $^1O_2$-Sensitive Linker.** Next, we investigated whether the reactivity toward $^1O_2$ is retained when methoxy groups in **5** are substituted for longer

**Scheme 2. Mechanism of $^1O_2$-Induced Decomposition of 9,10-Dialkoxyanthracene Linker (1)**[a]

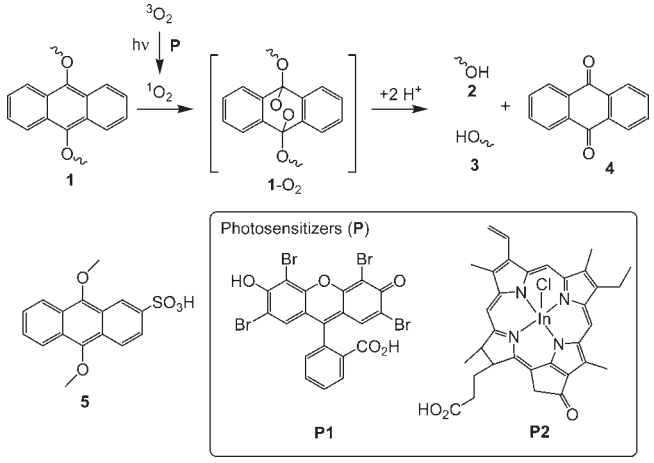


[a] Compound **5** is a commercially available representative derivative of 9,10-dialkoxyanthracene; **P1** is eosin (a green-light-absorbing photosensitizer); **P2** is $In^{3+}$(pyropheophorbide-*a*)Cl (a red-light-absorbing photosensitizer, a potential drug for photodynamic therapy[14]).

and functionalized groups. In particular, we prepared 9,10-di(3-hydroxypropoxy)anthracene **6** by alkylation of reduced in situ 9,10-anthraquinone with 3-iodopropan-1-ol (Scheme 3). Its overall yield over two steps was 20%. In the UV−visible spectrum of dialcohol **6**, characteristic peaks are observed in the region between 370 and 410 nm. These spectral features disappear in the presence of photogenerated $^1O_2$ (Figure S9, Supporting Information), indicating that compound **6** reacts with $^1O_2$. By using $^1H$ NMR spectroscopy and ESI mass spectrometry, we identified 9,10-anthraquinone **4** and 1,3-propanediol as products of this reaction (Figure 1).

Before synthesizing phosphoramidite **8** from dialcohol **6**, we studied whether the latter compound is stable under the conditions of DNA synthesis. In particular, we observed that **6** was not affected by oxidizer ($I_2$/water/pyridine) and deblocking ($Cl_3C$-$CO_2H$/$CH_2Cl_2$) solutions. Moreover, we found that it is stable in the deprotection solution (27% $NH_3$ in water) for at least 24 h.

Phosphoramidite **8** was obtained in two steps starting from **6**. First, dialcohol **6** was protected with 4,4′-dimethoxytrityl (DMT) group to obtain alcohol **7** (yield 40%), which was then converted to **8** (yield 43%; Scheme 3).[6] We observed that **8** can be coupled to primary alcohols in the presence of 1*H*-tetrazole with >95% yields (Experimental Section). Thus, building block **8** can be applied for linkage of a variety of molecular fragments under the conditions of DNA synthesis. This highly efficient


dx.doi.org/10.1021/ja108819c |*J. Am. Chem. Soc.* 2011, 133, 3972–3980

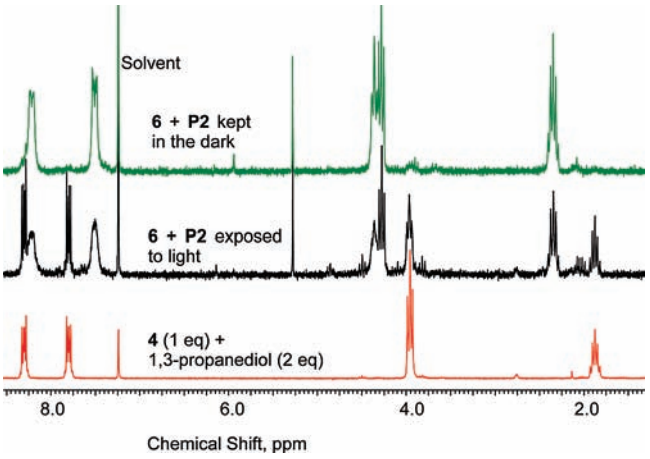


**Figure 1.** Monitoring cleavage of compound **6** (15 mM) in the presence of $^1O_2$ by $^1H$ NMR spectroscopy. Solvent was $CDCl_3$ containing 1% trifluoroacetic acid (v/v) and 0.1% DMSO (v/v). To generate $^1O_2$, photosensitizer **P2** (20 $\mu$M) was added to solutions of **6** and the resulting mixture was exposed to red light (2.6 mW) for 60 min.

chemistry allows generation of many complex molecules within a short time.

**A Fluorogenic Probe for Monitoring $^1O_2$ in Vitro.** Several excellent methods for $^1O_2$ monitoring in plant cells and whole plants have been reported.[8,15] In contrast, $^1O_2$ monitoring in live mammalian cells is less well established. This is not surprising because, in plant cells, large quantities of $^1O_2$ are generated in the chlorophyll-dependent process,[15] whereas substantially less $^1O_2$ can be produced in mammalian cells due to the absence of endogenous photosensitizers excitable by visible light. One well-studied exception is formation of large amount of $^1O_2$ during the oxidative burst in neutrophils.[16] $^1O_2$ generation in mammalian cells can be monitored by using either direct or indirect methods. The direct method is based on measuring weak phosphorescence of $^1O_2$ at 1270 nm,[8,15,17] It is not invasive and allows monitoring of $^1O_2$ in a single mammalian cell. However, to be able to conduct such a measurement, intracellular $H_2O$ should be substituted at least partially for $D_2O$ ($\geq$50% $D_2O$ is required).[17a,b] In the latter solvent lifetime of $^1O_2$ is substantially longer[18] and, consequently, more $^1O_2$ can be accumulated in the cell under these conditions. It has been reported that at least some types of cells can withhold such treatment for the time of the experiment. However, these are not exactly physiological conditions, and results obtained should be carefully extrapolated to $D_2O$-free conditions. Therefore, it would be very useful to be able to monitor $^1O_2$ formation directly in aqueous buffers. The data obtained in such experiments would be complementary to those obtained by the direct method. Several indirect methods applicable for monitoring $^1O_2$ in aqueous buffers have been reported. They are based on $^1O_2$-induced bleaching of photosensitizers (e.g., photofrin)[19] or chemical traps, such as 1,3-di(4-carboxyphenyl)isobenzofuran.[10] These methods are prone to false positive results, which can be caused, for example, by fluorescence quenching induced by intracellular components, aggregation of probes in the cell, or $^1O_2$-independent photobleaching of probes. In this case, interpretation of the data can become complicated. In contrast, fluorogenic ("light-up") $^1O_2$ probes generate the signal in the presence of $^1O_2$. They are highly specific for $^1O_2$, exhibit low background fluorescence, and are therefore highly sensitive. Known probes of this type include DMAX, DPAX,[13a]

**Scheme 3. Synthesis of Phosphoramidite 8**[a]

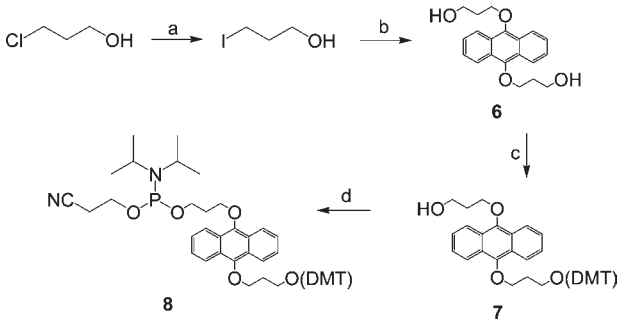


[a] (a) NaI, acetone; (b) 9,10-anthraquinone, $Na_2S_2O_4$, NaOH, Adogen 464; (c) 4,4′-dimethoxytrityl chloride, 4-(dimethylamino)pyridine, *N*,*N*′-diisopropylethylamine, pyridine; (d) 2-cyanoethyl *N*,*N*′-diisopropylchlorophosphoramidite.

commercially available singlet oxygen sensor green (SOSG),[13b] and MTTA−$Eu^{3+}$ complex.[13d] They all contain a 9,10-alkyl or aryl anthracene fragment, which binds singlet oxygen reversibly, forming a fluorescent product. We observed that this equilibrium is shifted toward the starting nonfluorescent probe in the presence of physiological concentrations of glutathione (5−10 mM; Figure S12, Supporting Information). This side reaction can hinder applications of the reversible anthracene-based $^1O_2$ probes in vivo.

It was claimed that MTTA−$Eu^{3+}$ can be applied for monitoring $^1O_2$ in live cells.[13d] The experimental conditions of the reported assay include incubation of HeLa cells in the serum-free medium containing a photosensitizer and a very high concentration of the $Eu^{3+}$ probe (0.4 mM). The incubation is followed by exposure of the cells to light over a long time (5 h). These are rather harsh conditions, which can cause cell death. No experimental evidence was provided in the original publication to show that HeLa cells survived this treatment.

We designed a fluorogenic $^1O_2$ probe (**11**), which consists of dyes F1 and F2 connected by 9,10-dialkoxyanthracene linker **1**. In contrast to known $^1O_2$ probes, **11** was expected to react with $^1O_2$ irreversibly (Scheme 2). Compound **11** was prepared by sequential coupling of phosphoramidite **8** (Scheme 3) and 5′-tetrachlorofluorescein-CE phosphoramidite on 3′-TAMRA CPG solid support (Figure 2). The coupling time was extended to 15 min to increase the reaction efficiency. The probe obtained was purified by high-performance liquid chromatography (HPLC). Its purity (>90%) was confirmed by analytical HPLC and its identity by matrix-assisted laser desorption ionization time-of-flight (MALDI-TOF) mass spectrometry (Figures S6 and S7, Supporting Information).

Analogously to **5** and **6** (Schemes 2 and 3), compound **11** reacts with photogenerated $^1O_2$ to form an unstable adduct that, according to HPLC and MALDI-TOF MS analysis, decomposes to form **12**, **13**, and **4** (Figures 2 and 3).

The fluorescence of both F1 and F2 in probe **11** is strongly quenched (Figure 4). Since the UV−visible spectrum of **11** cannot be reconstructed by superposition of the spectra of F1, F2, and **6** (Figure S10, Supporting Information), we concluded that the fluorophores interact with each other in their ground states. This indicates that the fluorescence quenching within **11** occurs at least in part via the contact mechanism.[20] Since both **12** and **13** are strongly fluorescent, $^1O_2$-induced conversion of **11** can be conveniently monitored by fluorescence spectroscopy and


dx.doi.org/10.1021/ja108819c |*J. Am. Chem. Soc.* 2011, 133, 3972–3980

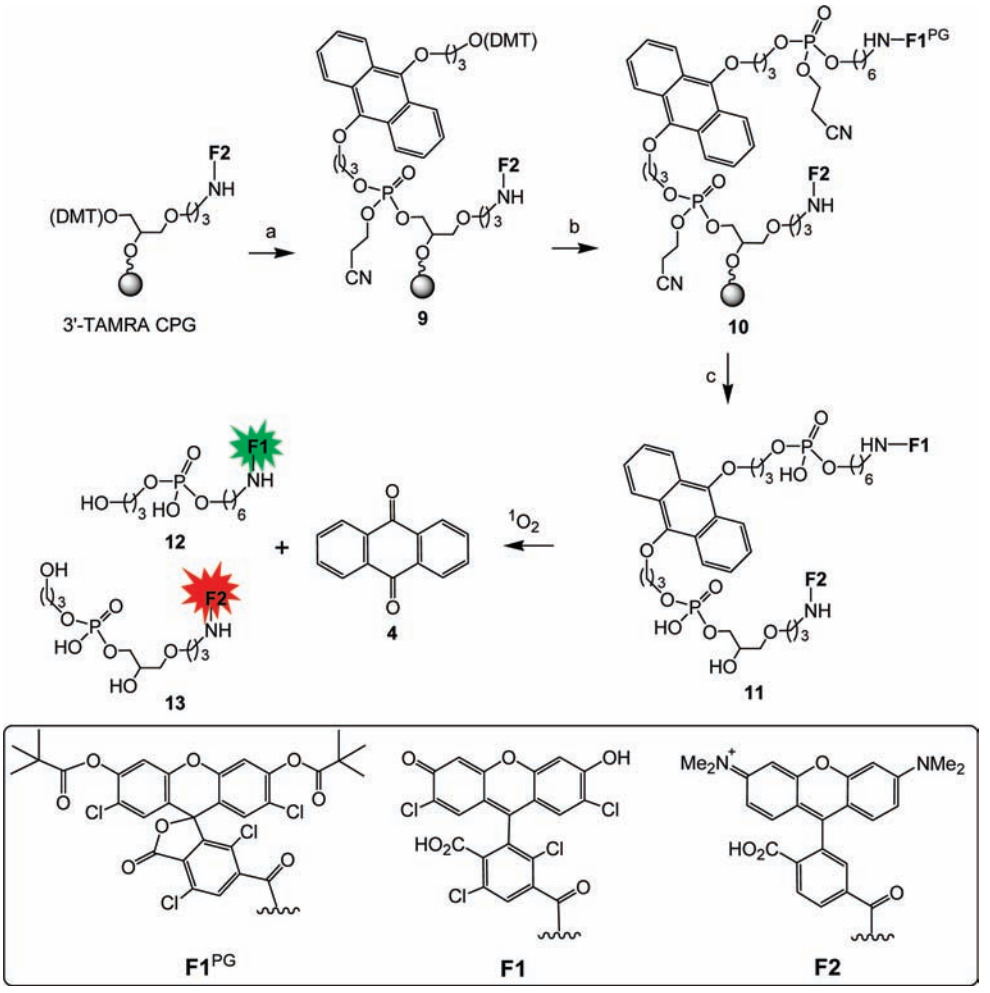


**Figure 2.** Synthesis and $^1O_2$-induced cleavage of fluorogenic probe **11**. (a) (1) $Cl_3CCO_2H$ in $CH_2Cl_2$ (3% v/v), (2) phosphoramidite **8**, 1*H*-tetrazole; (b) (1) $Cl_3CCO_2H$ in $CH_2Cl_2$ (3% v/v), (2) 6-[(4,7,2′,7′-tetrachloro-3′,6′-dipivaloylfluoresceinyl)carboxamido]hexyl 2-cyanoethyl *N*,*N*-diisopropyl-phosphoramidite (TET, Link Technologies), 1*H*-tetrazole; (c) aqueous $NH_3$ (27%).

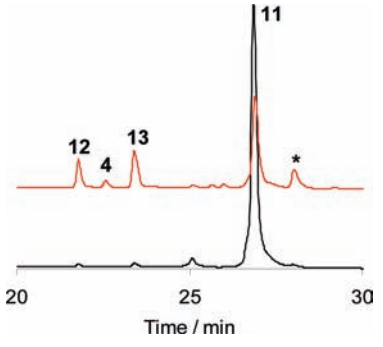


**Figure 3.** HPLC study of photocleavage of **11** (5 $\mu$M) at pH 7.0 in the presence of photosensitizer P2 (0.5 $\mu$M, red trace) or in its absence (black trace). Compound **11** was irradiated with red light (635 nm, 2.6 mW) for 60 min. A peak corresponding to photosensitizer P2 is indicated with an asterisk (*).

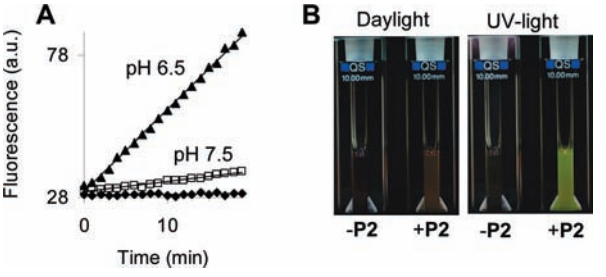


**Figure 4.** (A) Cleavage of probe **11** (5 $\mu$M) in the presence of P2 (0.1 equiv) and upon irradiation with red light (635 nm, 2.6 mW) at pH values indicated on the plot. The reaction was monitored by detecting the emission at $\lambda_{em}$ = 576 nm ($\lambda_{ex}$= 552 nm). Cleavage of **11** in the absence of **P2** was negligible (◆). Phosphate/citrate buffer (0.1 M) adjusted to the desired pH was used in all cases. Fluorescence intensity is given in arbitrary units. (B) Naked eye detection of $^1O_2$. Experimental conditions are the same as in panel A. pH = 7.5, irradiation time 50 min.

even by the naked eye (Figure 4). We observed that cleavage of **11** is facilitated at acidic pH (Figure 4A), which confirms the mechanism outlined in Scheme 2.

Probe **11** was found to be responsive not only to photogenerated $^1O_2$ but also to that generated as a result of thermal decomposition of the stable endoperoxide of 3,3′-(1,4-naphthylidene)dipropionate[21] ($NDPO_2$; Figure S11, Supporting Information). In particular, intensity of the fluorescence of **11** incubated for 120 min at 37 °C with $NDPO_2$ increased proportionally to the amount of $NDPO_2$ in the mixture.


dx.doi.org/10.1021/ja108819c |*J. Am. Chem. Soc.* 2011, 133, 3972–3980

Probe **11** is specific to $^1O_2$. In particular, the increase in relative fluorescence intensity of **11** induced by $^1O_2$ $[(F - F_0)/F]$ is 6.2. Among other studied reactive species ($H_2O_2$, $HO^•$, $O_2^-$, $ClO^-$, NO), only $ClO^-$ anion affected the fluorescence of **11** to some extent: $(F - F_0)/F = 0.7$, and the $^1O_2$ selectivity of **11** with respect to $ClO^-$ anion is equal to a factor of 9. For other reagents the selectivity is better than a factor of 15 (Figure 5). The $^1O_2$ specificity of our probe is comparable to that of MTTA−$Eu^{3+}$, which was applied earlier for detection of $^1O_2$ in mammalian cells.[13d] In particular, the increase in relative fluorescence intensity of MTTA−$Eu^{3+}$ induced by $^1O_2$ $[(F - F_0)/F]$ is ∼4.3. The effect of $ClO^-$ anion on MTTA−$Eu^{3+}$ was not studied. The $^1O_2$ selectivity of MTTA−$Eu^{3+}$ with respect to hydrogen peroxide and hydroxyl radicals is ∼15.

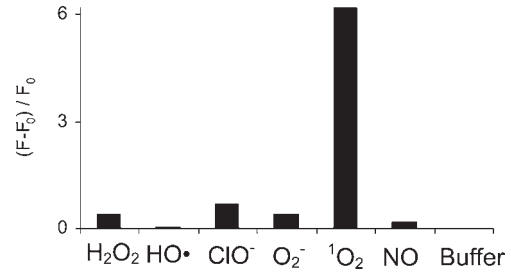


**Figure 5.** Increase in relative fluorescence intensity ($\lambda_{ex}$ = 552 nm, $\lambda_{em}$ = 576 nm) of **11** (5 $\mu$M) in the presence of reactive oxygen and nitrogen species indicated on the horizontal axis. $F$ = fluorescence of **11** after addition of ROS/RNS and incubation for 60 min; $F_0$ = fluorescence of the same solution before addition of ROS/RNS. $^1O_2$ was generated by exposure of P2[14] (0.5 $\mu$M) to red light (635 nm, 2.6 mW) for 60 min. $c(H_2O_2)$ = 100 $\mu$M. $OH^•$ was generated from $H_2O_2$ (100 $\mu$M) and $Cu^{2+}$ (10 $\mu$M). $c$(NaOCl) = 3 $\mu$M. NO was generated from *S*-nitrosocysteine (1 mM).[22] $O_2^-$ was generated from the reaction of xanthine (100 $\mu$M) and xanthine oxidase (40 milliunits/mL).[23] Buffer was citrate/phosphate (0.1 M, pH 7.0); $T$ = 22 °C.

**Application of the Fluorogenic Probe for Monitoring $^1O_2$ in Live Cells.** We investigated the cellular permeability of probe **11** in human leukemia HL-60 cells by using flow cytometry. Two emission filters were applied (FL1, 530 ± 30 nm; FL2, 585 ± 40 nm) that allowed us to detect the fluorescence of F1 and F2 dyes separately from each other. We observed that, upon treatment of the cells with **11**, their mean fluorescence was increased only by a factor of 1.3 (FL1 channel) and 1.1 (FL2 channel), which indicated that very little **11** went through the membrane. Thus, though **11** is an excellent probe for detecting $^1O_2$ in vitro (Figure 4), it is not suitable for in vivo application.

To improve its membrane permeability, we attached a hydrophobic cholesterol residue to probe **11** (creating probe **16**)

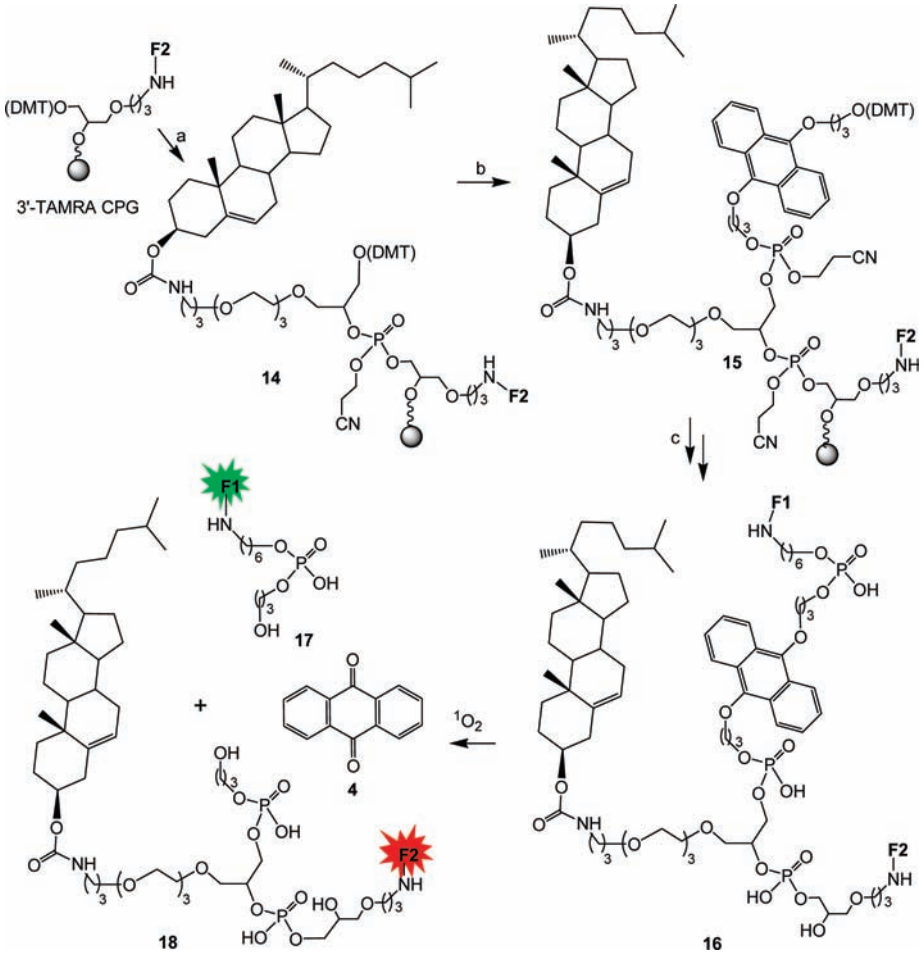


**Figure 6.** Synthesis of cell-permeable, fluorogenic $^1O_2$ probe **16**. (a) (1) $Cl_3CCO_2H$ in $CH_2Cl_2$ (3% v/v), (2) cholesteryl-TEG phosphoramidite (Glen Research), 1*H*-tetrazole; (b) (1) $Cl_3CCO_2H$ in $CH_2Cl_2$ (3% v/v); (2) phosphoramidite **8**, 1*H*-tetrazole; (c) (1) $Cl_3CCO_2H$ in $CH_2Cl_2$ (3% v/v), (2) 6-[(4,7,2′,7′-tetrachloro-3′,6′-dipivaloylfluoresceinyl)carboxamido]hexyl 2-cyanoethyl *N*,*N*-diisopropylphosphoramidite (TET, Link Technologies), 1*H*-tetrazole; (3) aqueous $NH_3$ (27%).


dx.doi.org/10.1021/ja108819c |*J. Am. Chem. Soc.* 2011, 133, 3972–3980

(Figure 6). Synthesis of probe **16** was conducted by sequential coupling of cholesteryl-TEG phosphoramidite, phosphoramidite **8** (Scheme 3), and 5′-tetrachlorofluorescein-CE phosphoramidite on 3′-TAMRA CPG solid support (Figure 6). In contrast to **11**, probe **16** permeates cellular membranes well. In particular, the mean fluorescence of the cells treated with **16** was over 1 order of magnitude higher than that of the untreated cells. To test whether probe **16** is responsive to $^1O_2$, we loaded cells with P2 (50−200 nM) and exposed them to red light for <25 min. Under these conditions, $^1O_2$ is generated at nontoxic concentrations.[10] We observed that **16** is decomposed upon formation of $^1O_2$, which is reflected in the substantial increase in mean fluorescence of HL-60 cells (Figure 7). Interestingly, the increase in fluorescence intensity of F2 (factor of 14.3, FL2 channel) was significantly larger than that one of F1 (factor of 3.3, FL1 channel). At the same time we observed that $^1O_2$-induced decomposition of **16** in cells leads to the substantial increase in fluorescence signal characteristic for F1 in the medium (Figure 8). These data allowed us to conclude that product **17** containing F1 is transported out of the cells after its generation, whereas product **18** carrying F2 stays inside, probably due to the cholesteryl fragment (Figure 6). Thus, the $^1O_2$ detection assay based on probe **16** does not require rather expensive flow cytometers but can be monitored by using more accessible and cheap fluorescence spectrophotometers or fluorescence readers. We also confirmed that neither P2 nor probe **16** nor their mixture causes cell death under our experimental conditions (Figure S13, Supporting Information).

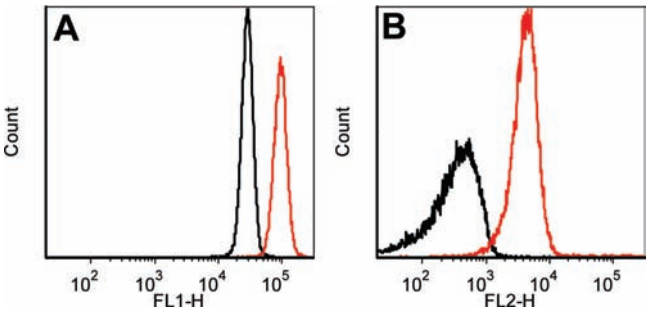


**Figure 7.** Fluorescence of HL-60 cells loaded with **16** ($c_{medium}$ = 3 $\mu$M) and exposed to red light for 20 min. Black traces, no P2 was added; red traces, cells were loaded with P2 ($c_{medium}$ = 200 nM). Fluorescence intensity of individual cells is plotted versus the number of cells. Excitation was at 488 nm. (A) FL1-H is the intensity of emission at 530 ± 30 nm; (B) FL2-H is the intensity of emission at 585 ± 40 nm.

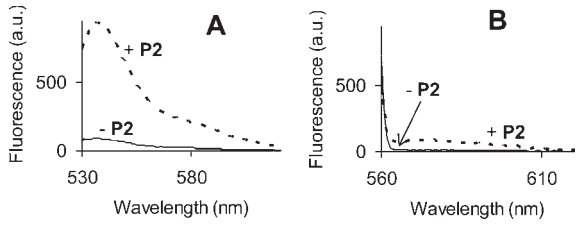


**Figure 8.** Fluorescence spectra of the medium, where HL-60 cells were loaded with probe **16** ($c_{medium}$ = 3 $\mu$M) and exposed to red light (20 min). The spectra were obtained with cells loaded (+P2, $c_{medium}$ = 200 nM) and not loaded (−P2) with the photosensitizer as indicated on plots. (A) Detection of fluorophore F1 ($\lambda_{ex}$ = 519 nm); (B) detection of fluorophore F2 ($\lambda_{ex}$ = 552 nm).

Further on, we investigated whether probe **16** reacts with $^1O_2$ generated in its own cell or it can also react with $^1O_2$ diffusing from other cells. In this experiment we separated cells into two equally large populations and loaded one of them with photosensitizer P2. Then cells in both populations were mixed together, incubated with probe **16**, washed, exposed to red light, and analyzed by flow cytometry (Figure 9). Since photosensitizer P2 fluoresces in the far-red region,[10] which does not overlap with fluorescence of **16**, **17**, and **18**, the cells loaded and not loaded with P2 can be easily distinguished from each other even in mixtures. We observed that **16** is cleaved only in cells that contain photosensitizer P2 (compare plots in Figure 9B,C), which indicates that under our experimental conditions the lifetime of $^1O_2$ is too short to migrate from one cell to another. These results are in good agreement with the data of Ogilby and co-workers,[24] obtained by using the direct method of $^1O_2$ detection. In particular, they have estimated that the distance traveled by $^1O_2$ after its generation in the cell is equal to ~270 nm. Since the diameter of a typical mammalian cell is >10 $\mu$m, $^1O_2$ generated in the cell is not expected to leave it.

**Red-Light-Activated "Caged" Oligodeoxyribonucleotides.** We designed an inactive ("caged") reagent as a duplex consisting of two oligodeoxyribonucleotides: ODN1 and ODN4 (Figure 10). ODN4 is a strand that was supposed to bind to the target nucleic acid after activation of the "caged" reagent. ODN1 is a blocker sequence. It binds tightly to ODN4, forming the stable "caged" reagent ODN1/ODN4 duplex. ODN1 contains linker **1** in its interior (Figure 10). This linker is cleaved fully within 40 min in the presence of photosensitizer P2 (0.1 equiv) and upon illumination with red light (Figure 10A, black trace). Under similar experimental conditions the activation of "caged" ODNs based on the

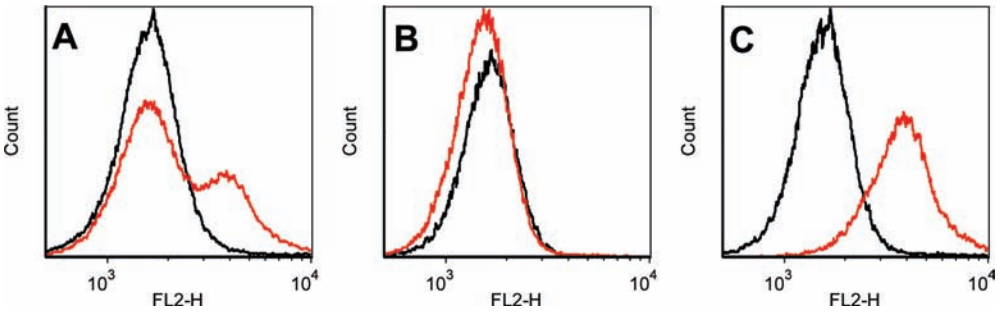


**Figure 9.** Equal numbers of cells loaded and not loaded with photosensitizer P2 (concentration in the medium was 1 $\mu$M) were mixed together, incubated with **16** (concentration in the medium was 1 $\mu$M), washed, and placed in the medium. Black traces, cells kept in the dark; red traces, cells irradiated for 20 min with red light. (A) No gating; (B) gating on cells that do not contain P2; (C) gating on cells that contain P2. FL2 is the intensity of emission at 585 ± 40 nm.


dx.doi.org/10.1021/ja108819c | J. Am. Chem. Soc. 2011, 133, 3972–3980

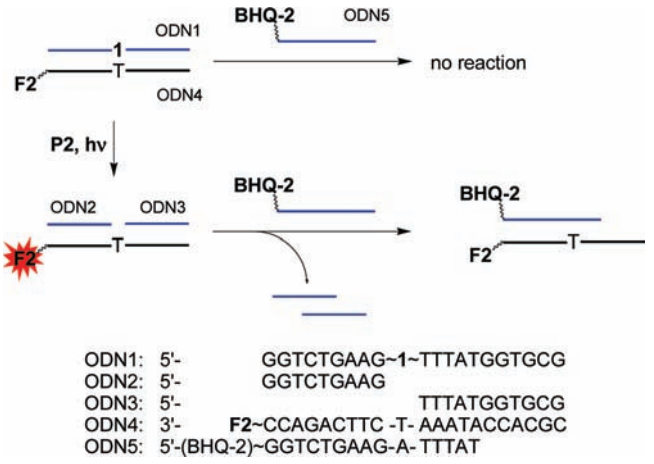


**Figure 10.** Outline of red-light-induced triggering of hybridization ability of ODNs. The structure of F2 is shown in Figure 2. BHQ-2 = black hole quencher 2; $h\nu$ = red light.

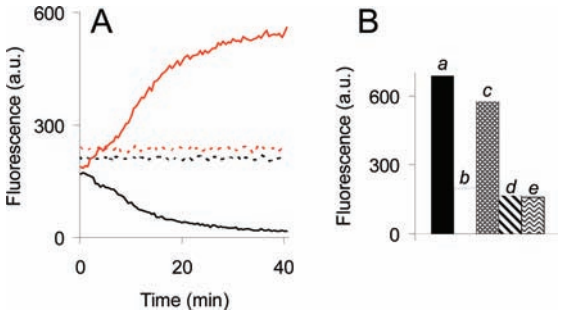


**Figure 11.** (A) Monitoring photocleavage of linker **1** in ODN1/ODN4 duplex (10 $\mu$M) in citric acid/phosphate buffer (0.1 M, pH 5) at 22 °C in the presence of P2 (1 $\mu$M, solid lines) and in its absence (dotted lines). Red lines, $\lambda_{ex}$ = 400 nm and $\lambda_{em}$ = 583 nm (emission of F2, Figure 2A); black lines, $\lambda_{ex}$ = 400 nm and $\lambda_{em}$ = 450 nm (emission of linker **1**, Scheme 2). (B) Fluorescence intensities ($\lambda_{ex}$ = 400 nm, $\lambda_{em}$ = 583 nm; emission of F2) were measured in citric acid/phosphate buffer (0.1 M) at 22 °C in the presence of P2 (1 $\mu$M). Concentrations of ODNs were 10 $\mu$M. (a) ODN4, kept in the dark for 40 min; (b) ODN1/ODN4, kept in the dark for 40 min; (c) ODN1/ODN4, exposed to red light for 40 min; (d) ODN5 added to solution from case c; (e) ODN4/ODN5.

~SCH=CHS~ linker occurs with less than 10% yield.[6,7] To achieve a sufficient yield of uncaging of these older "caged" ODNs, high concentrations of photosensitizers and long irradiation times have to be applied. However, these conditions are damaging to cells. As a result of cleavage of linker **1** in the "caged" reagent ODN1/ODN4, an unstable duplex (ODN2, ODN3)/ODN4 is formed. This compound decomposes spontaneously under our experimental conditions (see caption to Figure 11) with formation of single-stranded ODN4.

We labeled the 3′-terminus of ODN4 with fluorophore F2 to be able to monitor the processes of formation and decomposition (activation) of the "caged" reagent by fluorescence spectroscopy. In particular, we observed that in the "caged" state the fluorescence of F2 (ODN4) is quenched due to its proximity to linker **1** (ODN1), whereas in the uncaged state the fluorescence of F2 is restored (Figure 11A, red trace). Addition of a target nucleic acid labeled at its 5′-terminus with black hole quencher 2 (ODN5) to the "uncaged" reagent leads to quenching of the fluorescence of F2 due to formation of duplex ODN4/ODN5 (Figures 10 and 11B). In contrast, a target nucleic acid (ODN5) cannot substitute ODN1 in the "caged" reagent since the sequence of ODN5 was selected to be six nucleotides shorter than that of ODN1. Thus, red light acts as an efficient trigger of hybridization of the "caged" reagent to the nucleic acid target.

## CONCLUSIONS

We developed a linker based on a 9,10-dialkoxyanthracene structure. It is cleaved with high yield in the presence of $^1O_2$. On the basis of this linker, we prepared the fluorogenic ("light-up") probe for monitoring $^1O_2$ in live mammalian cells. By using this probe we confirmed that $^1O_2$ after its generation does not diffuse to other cells, which is an indication of its short lifetime in the cellular milieu under our experimental conditions. These results are in good agreement with the data of Ogilby and co-workers[24] obtained by the direct method of $^1O_2$ detection.

We also applied the new linker to prepare red-light-activated "caged" oligodeoxyribonucleotides. Analogous reagents reported before contain ~SCH=CHS~ linkers reacting with $^1O_2$ via an inefficient [2 + 2] addition mechanism.[6,7] Consequently, the reaction between the ~SCH=CHS~ and $^1O_2$ is rather slow. Under physiological conditions and in the presence of $^1O_2$, the ~SCH=CHS~ moiety is quickly oxidized with formation of stable sulfoxides that are not further cleaved by $^1O_2$. This side reaction reduces the efficiency of the uncaging process. In contrast, the anthracene-based linker described here reacts with $^1O_2$ quickly, since this process is a highly efficient [4 + 2] addition. Moreover, this linker is cleanly converted by $^1O_2$ to the desired cleavage products without any significant side reactions.

Previously, we have demonstrated that $^1O_2$-sensitive linkers can be applied for chemical modification of predefined regions on DNA nanostructures.[11] Since the linker reported here reacts with $^1O_2$ quickly and generates cleavage products with high yield, its application may reduce the time of DNA exposure to highly reactive $^1O_2$ that can possibly preserve the DNA scaffold intact over many steps of the surface modification. Possible applications of the new photocleavable linker in DNA nanotechnology are currently being investigated in our laboratories and those of our cooperation partners. The first preliminary results of these studies have been recently published.[25]

## EXPERIMENTAL SECTION

Commercially available chemicals of the best quality from Aldrich/Sigma/Fluka (Germany) were obtained and used without purification. Phosphoramidites and controlled pore glass (CPG) solid support were from Glen Research (United States) and Link Technologies (United Kingdom). An indicator of dead cells, TO-PRO-3 iodide, was purchased from Invitrogen. MALDI-TOF mass spectra were recorded on a Bruker Biflex III spectrometer. The matrix mixture (2:1 v/v) was prepared from 6-aza-2-thiothymine (ATT, saturated solution in acetonitrile) and diammonium citrate (0.1 M in water). Samples for mass spectrometry were prepared by the dried-droplet method by using a 1:2 probe/matrix ratio. Mass accuracy with external calibration was 0.1% of the peak mass, that is, ±2.0 at $m/z$ 2000. HPLC was performed at 22 °C on a Shimadzu liquid chromatograph equipped with a UV detector and a Macherey−Nagel Nucleosil C4 250 × 4.6 mm column. HPLC gradient (solution A, 0.1 M ($NEt_3H$)(OAc); solution B, $CH_3CN$) was 0% B for 5 min and then from 0% to 90% in 40 min. UV−vis spectra were


dx.doi.org/10.1021/ja108819c |J. Am. Chem. Soc. 2011, 133, 3972–3980

measured on a Varian Cary 100 Bio UV−vis spectrophotometer by using 1 cm optical path black-wall absorption semimicrocuvettes (Hellma GmbH, Germany) with a sample volume of 0.7 mL. These cuvettes were also used for photochemical experiments. Light from different light sources was applied from the top of the cuvette via an optical fiber. Fluorescence spectra were acquired on a Varian Cary Eclipse fluorescence spectrophotometer by using black-wall fluorescence semimicrocuvettes (Hellma GmbH, Germany) with a sample volume of 0.7 mL. The fluorescence of compounds **11**, **12**, **13**, **17**, **18**, and P2 in live HL-60 cells was quantified by use of an Accuri C6 Flow cytometer. The data were processed by use of the CFlow Plus (Accuri) and FCS Express V3 software packages.

**Synthesis.** *3-Iodo-1-propanol*[26]. A mixture of 3-chloro-1-propanol (14.6 g, 158 mmol) and NaI (47.3 g, 315 mmol) in acetone (100 mL) was refluxed overnight. The solution was filtered and the solvent was removed by evaporation. The residue was redissolved in $CH_2Cl_2$, filtered and the solvent removed. The resulting red-orange oil was redissolved again in $CH_2Cl_2$ (25 mL) and filtered through a silica plug. The solvent was evaporated and the resulting red-orange oil was used in the next step without additional purification. Yield 20.8 g, 72%; $R_f$ (ethyl acetate/$CH_2Cl_2$ 1/3 v/v) = 0.51. $^1$H NMR (200 MHz, $CDCl_3$), $\delta$ in ppm: 3.74 (t, 2H, $^3J$ = 5.9 Hz), 3.30 (t, 2H, $^3J$ = 6.8 Hz), 2.04 (m, 2H).

*9,10-Bis(3-hydroxypropyloxy)anthracene*[27] (***6***). Nitrogen-saturated water (150 mL) and $CH_2Cl_2$ (150 mL) were added to a mixture of 9,10-anthraquinone (2.57 g, 12.36 mmol), $Na_2S_2O_4$ (4.3 g, 24.7 mmol), and Adogen 464 (4.64 g, 10 mmol). The mixture was stirred for 5 min and then NaOH (4.94 g, 123.5 mmol) was added. Stirring was continued for 10 min and 3-iodo-1-propanol (11.5 g, 61.8 mmol) was added dropwise. The mixture was stirred overnight at 22 °C. The reaction completion was confirmed by thin-layer chromatography (TLC). Then the phases were separated and the water phase was washed with $CH_2Cl_2$. The combined organic phases were washed with water and dried over $MgSO_4$. The solution volume was reduced to 40 mL and the product was precipitated overnight at −25 °C. The yellow solid obtained was dried in vacuo and then purified by column chromatography with a mixture of ethyl acetate/$CH_2Cl_2$ (1/4 v/v). Yield 1.13 g, 28%; $R_f$ (ethyl acetate/$CH_2Cl_2$ 1/3 v/v) = 0.33. $^1$H NMR (200 MHz, DMSO-$d_6$), $\delta$ in ppm: 8.27 (dd, 4H, $J$ = 6.8, 3.2 Hz), 7.55 (dd, 4H, $J$ = 6.8, 3.2 Hz), 4.66 (t, 2H, $^3J$ = 5.1 Hz), 4.20 (t, 4H, $^3J$ = 6.4 Hz), 3.79 (m, 4H), 2.13 (m, 4H).

*3-(10-{3-[Bis(4-methoxyphenyl)phenylmethoxy]propyloxy}anthracen-9-yloxy)propan-1-ol* (***7***). Compound **6** (1.13 g, 3.46 mmol) was dissolved in anhydrous pyridine (15 mL), and 4-(dimethylamino)pyridine (0.34 g, 2.77 mmol) and *N*,*N*-diisopropylethylamine (0.36 mg, 0.48 mL, 2.77 mmol) were added. A solution of 4,4′-dimethoxytrityl chloride (1.41 g, 4.16 mmol) in anhydrous pyridine (15 mL) was prepared separately and then added dropwise to the first solution. The resulting mixture was stirred for 2 h at 22 °C. Then pyridine was removed at reduced pressure (0.01 mbar) and MeOH (10 mL) was added. After 15 min the mixture was poured into saturated $NaHCO_3$ solution and extracted with $CH_2Cl_2$ (3 × 10 mL). The combined organic phases were dried ($MgSO_4$) and the solvent was evaporated. The residue left was dissolved in $CH_2Cl_2$ (15 mL) and purified by column chromatography with a mixture of ethyl acetate/$CH_2Cl_2$ (1/25 v/v) containing 1% triethylamine to give the final compound (0.87 g, 40%) as a light yellow oil. $R_f$ = 0.50 [ethyl acetate/$CH_2Cl_2$ 1/25 (v/v) containing 1% triethylamine]. $^1$H NMR (200 MHz, acetone-$d_6$), $\delta$ in ppm: 8.30 (dd, 4H, $J$ = 15.6, 8.2 Hz), 7.57−7.23 (m, 13H), 6.90 (m, 4H), 4.36 (t, 2H, $^3J$ = 6.0 Hz), 4.30 (t, 2H, $^3J$ = 6.5 Hz), 3.98 (t, 2H, $^3J$ = 5.0 Hz) 3.78 (s, 6H), 3.54 (t, 2H, $^3J$ = 5.2 Hz), 2.36 (m, 2H), 2.24 (m, 2H). $^{13}$C NMR (50 MHz, acetone-$d_6$), $\delta$ in ppm: 31.77, 34.39, 55.49, 59.07, 60.94, 73.40, 73.65, 86.94, 113.90, 123.53, 125.97, 126.01, 126.23, 127.52, 128.62, 129.00, 130.94, 137.33, 146.59, 148.04, 148.29, 159.60.

*3-(10-{3-[Bis(4-methoxyphenyl)phenylmethoxy]propyloxy}anthracen-9-yloxy)propyl 2-Cyanoethyl N,N-diisopropylphosphoramidite* (***8***). Compound **7** (302 mg, 0.48 mmol) and *N*,*N*-diisopropylethylamine (0.28 g, 0.38 mL, 2.16 mmol) were dissolved in anhydrous $CH_2Cl_2$ (10 mL). Then 2-cyanoethyl *N*,*N*-diisopropylchlorophosphoramidite (0.23 g, 0.96 mmol) was slowly added while stirring. The reaction mixture was stirred for 2 h at 22 °C and then poured into 30 mL of saturated $NaHCO_3$ solution and extracted with $CH_2Cl_2$ (3 × 10 mL). The combined organic phases were dried over $Na_2SO_4$ and the solvent was evaporated. The resulting oil was purified by column chromatography with hexane/$CH_2Cl_2$ (2/1 v/v) containing 1% triethylamine to give the final compound (0.17 g, 43%) as a light yellow oil; $R_f$ = 0.53 [hexane/$CH_2Cl_2$ 2/1 (v/v) containing 1% triethylamine]. $^1$H NMR (400 MHz, acetone-$d_6$), $\delta$ in ppm: 8.34 (m, 4H), 7.55 (m, 4H), 7.44−7.39 (m, 6H), 7.33 (t, 2H, $^3J$ = 7.6 Hz), 7.24 (t, 1H, $^3J$ = 7.4 Hz), 6.90 (m, 4H), 4.37 (t, 2H, $^3J$ = 6.0 Hz), 4.32 (t, 2H, $^3J$ = 6.5 Hz), 4.17−4.04 (m, 2H), 3.95−3.84 (m, 2H) 3.77 (s, 6H), 3.75−3.67 (m, 2H), 3.54 (t, 2H, $^3J$ = 6.0 Hz), 2.77 (t, 2H, $^3J$ = 6.2 Hz), 2.36 (m, 4H), 1.21 (m, 12H). $^{13}$C NMR (50 MHz, acetone-$d_6$), $\delta$ in ppm: 20.76, 20.89, 24.87, 24.91, 25.01, 25.06, 31.78, 33.09, 43.67, 43.91, 55.50, 59.30, 59.67, 60.95, 73.00, 73.43, 86.94, 113.90, 123.52, 123.58, 125.98, 126.26, 126.29, 127.52, 128.62, 129.00, 130.94, 137.33, 146.59, 148.12, 148.14, 159.60. $^{31}$P NMR (160 MHz, acetone-$d_6$), $\delta$ in ppm: 147.44.

**Photogeneration of $^1O_2$.** $^1O_2$ was generated by using two photosensitizers: eosin (P1) and $In^{3+}$(pyropheophorbide-*a*)chloride (P2) (Scheme 2). P1 was irradiated with green light [mercury lamp (150 W) combined with green light filter (500−550 nm)], whereas P2 was irradiated with red light (red laser, 635 nm, 2.6 mW). P2 was used in all experiments with live cells.

**Synthesis of Fluorogenic $^1O_2$ Probes and ODN1.** Probes **11** and **16** and oligodeoxyribonucleotide ODN1 were prepared on a DNA/RNA synthesizer with a commercially available 3′-TAMRA CPG solid support and 5′-tetrachlorofluorescein-CE phosphoramidite (both purchased from Link Technologies, United Kingdom), cholesteryl-TEG phosphoramidite (Glen Research, United States), and phosphoramidite **8** (Figures 2, 6). Coupling time in each case was extended to 15 min. Oxidation of P(III) derivatives ($I_2$, pyridine) and removal of 4,4′-dimethoxytrityl group ($CCl_3CO_2H$) were conducted under standard conditions usually applied in DNA synthesis.

*Compound* ***11***. Phosphoramidite **8** was first coupled to the solid support 3′-TAMRA CPG (1 $\mu$mol scale). After the oxidation step and removal of 4,4′-dimethoxytrityl group, 5′-tetrachlorofluorescein-CE phosphoramidite was coupled and 4,4′-dimethoxytrityl group was cleaved. The final product was cleaved from the support and fully deprotected by treatment with aqueous $NH_3$ solution (27%) at 55 °C for 2 h. The resulting crude compound was purified by reversed-phase HPLC. Yield 71%; HPLC $R_t$ = 28.0 min; MALDI-TOF MS, negative mode, calculated for $C_{78}H_{75}C_{l4}N_4O_{22}P_2$ $[M - H]^-$, $m/z$ 1623.3; found,1623.0.

*Compound* **16**. Cholesteryl-TEG phosphoramidite was first coupled to the solid support 3′-TAMRA CPG (1 μmol scale). After the oxidation step and removal of 4,4′-dimethoxytrityl group, phosphoramidite **8** followed by 5′-tetrachlorofluorescein-CE phosphoramidite were coupled and the terminal 4,4′-dimethoxytrityl group was removed. The final product was cleaved from the support and fully deprotected by treatment with aqueous $NH_3$ solution (27%) at 55 °C for 2 h. The resulting crude compound was purified by reversed-phase HPLC. Yield 60%; HPLC $R_t$ = 40.0 min; MALDI-TOF MS, negative mode, calculated for $C_{118}H_{145}Cl_4N_5O_{32}P_3$ $[M - H]^-$, $m/z$ 2379.8; found, 2377.8.

*ODN1*. Yield 30%. MALDI-TOF MS (negative mode) calculated for $C_{218}H_{268}N_{75}O_{128}P_{20}$ $[M - H]^-$, 6603.2; found, 6599.6.

## ■ ASSOCIATED CONTENT

**Supporting Information.** Fifteen figures, showing NMR, MALDI-TOF, and UV−visible spectra of new compounds as well as results of additional studies not included in the main text. This material is available free of charge via the Internet at http://pubs.acs.org.

## ■ AUTHOR INFORMATION

**Corresponding Author**
Andriy.Mokhir@urz.uni-heidelberg.de

## ■ ACKNOWLEDGMENT

We thank the Deutsche Forschungsgemeinschaft (DFG MO 1418/1-2 and 1-3) and Ruprecht-Karls-Universität Heidelberg (ZUK49/1 TP 10.10) for financial support.

## ■ REFERENCES

(1) Recent reviews on "caged" reagents: (a) Lemke, E. A. *ChemBioChem* **2010**, *11*, 1825. (b) Deiters, A. *ChemBioChem* **2010**, *11*, 47. (c) Casey, J. P.; Blidner, R. A.; Monroe, W. T. *Mol. Pharmaceutics* **2009**, *6*, 669. (d) Lee, H. M.; Larson, D. R.; Lawrence, D. S. *ACS Chem. Biol.* **2009**, *4*, 409. (e) Young, D. D.; Deiters, A. *Org. Biomol. Chem.* **2007**, *5*, 999. (f) Tang, X.; Dmochowski, I. J. *Mol. Biosyst.* **2007**, *3*, 100. (g) Mayer, G.; Heckel, A. *Angew. Chem., Int. Ed.* **2006**, *45*, 4900. (h) Furuta, T.; Noguchi, K. *Trends Anal. Chem.* **2004**, *23*, 511. (i) Curley, K.; Lawrence, D. S. *Curr. Opin. Chem. Biol.* **1999**, *3*, 84.

(2) (a) Richards, J. L.; Seward, G. K.; Wang, Y.-H.; Dmochowski, I. J. *ChemBioChem* **2010**, *11*, 320. (b) Tang, X. J.; Swaminathan, J.; Gewirtz, A. M.; Dmochowski, I. J. *Nucleic Acids Res.* **2008**, *36*, 559. (c) Tang, X. J.; Maegawa, S; Weinberg, E. S.; Dmochowski, I. J. *J. Am. Chem. Soc.* **2007**, *129*, 11000.

(3) Meunier, J.-R.; Sarasin, A.; Marrot, L. *Photochem. Photobiol.* **2002**, *75*, 437.

(4) Monroe, W. T.; McQuain, M. M.; Chang, M. S.; Alexander, J. S.; Haselton, F. R. *J. Biol. Chem.* **1999**, *274*, 20895.

(5) Baugh, S. D. P.; Yang, Z.; Leung, D. K.; Wilson, D. M.; Breslow, R. *J. Am. Chem. Soc.* **2001**, *123*, 12488.

(6) Rotaru, A.; Mokhir, A. *Angew. Chem., Int. Ed.* **2007**, *46*, 6180.

(7) Rotaru, A.; Kovács, J.; Mokhir, A. *Bioorg. Med. Chem. Lett.* **2008**, *18*, 4336.

(8) (a) Hackbarth, S.; Schlothauer, J.; Preuss, A.; Röder, B. *J. Photochem. Photobiol. B* **2010**, *98*, 173. (b) Adam, W.; Kazakov, D. V.; Kazakov, V. P. *Chem. Rev.* **2005**, *105*, 3371.

(9) (a) Frimer, A. A. *Chem. Rev.* **1979**, *79*, 359. (b) Clennan, E. L.; Nagraba, K. *J. Am. Chem. Soc.* **1988**, *110*, 4312. (c) Kearns, D. R. *Chem. Rev.* **1971**, *71*, 395. (d) Foote, C. S. *Pure Appl. Chem.* **1971**, *27*, 635.

(10) Arian, D.; Cló, E.; Gothelf, K. V.; Mokhir, A. *Chem.—Eur. J.* **2010**, *16*, 288.

(11) Voigt, N. V.; Tørring, T.; Rotaru, A.; Jacobsen, M. F.; Ravnsbæk, J. B.; Subramani, R.; Mamdouh, W.; Kjems, J.; Mokhir, A.; Besenbacher, F.; Gothelf, K. V. *Nat. Nanotechnol.* **2010**, *5*, 200.

(12) Rothemund, P. W. K. *Nature* **2006**, *440*, 297.

(13) (a) Tanaka, K.; Miura, T.; Umezawa, N.; Urano, Y.; Kikuchi, K.; Higuchi, T.; Nagano, T. *J. Am. Chem. Soc.* **2001**, *123*, 2530. (b) Ragàs, X.; Jiménez-Banzo, A.; Sánchez-García, D.; Batllori, X.; Nonell, S. *Chem. Commun.* **2009**, 2920. (c) Nardello, V.; Aubry, J.-M.; Johnston, P.; Bulduk, I.; de Vries, A. H. M.; Alsters, P. L. *Synlett.* **2005**, *17*, 2667 and references therein. (d) Song, B.; Wang, G.; Tan, M.; Yuan, J. *J. Am. Chem. Soc.* **2006**, *128*, 13442.

(14) Chen, Y.; Zheng, X.; Dobhal, M. P.; Gryshuk, A.; Morgan, J.; Dougherty, T. J.; Oseroff, A.; Pandey, R. K. *J. Med. Chem.* **2005**, *48*, 3692.

(15) Hideg, É. *Centr. Eur. J. Biol.* **2008**, *3*, 273.

(16) Steinbeck, M. J.; Khan, A. U.; Karnovsky, M. *J. Biol. Chem.* **1992**, *267*, 13425.

(17) (a) Breitenbach, T.; Kuimova, M. K.; Gbur, P.; Hatz, S.; Bitsch Schack, N.; Wett Pedersen, B.; Lambert, J. D.C.; Poulsen, L.; Ogilby, P. R. *Photochem. Photobiol. Sci.* **2009**, *8*, 442. (b) Hatz, S.; Lambert, J. D. C.; Ogilby, P. R. *Photochem. Photobiol. Sci.* **2007**, *6*, 1106. (c) Jiménez-Banzo, A.; Sagristà, M. L.; Mora, M.; Nonell, S. *Free Radical Biol. Med.* **2008**, *44*, 1926. (d) Jarvi, M. T.; Niedre, M. J.; Patterson, M. S.; Wilson, B. C. *Photochem. Photobiol.* **2006**, *82*, 1198. (e) Oelckers, S.; Ziegler, T.; Michler, T.; Röder, B. *J. Photochem. Photobiol. B* **1999**, *53*, 121.

(18) Ogilby, P. R.; Foote, C. S. *J. Am. Chem. Soc.* **1983**, *105*, 3423.

(19) Dysart, J. S.; Patterson, M. S. *Phys. Med. Biol.* **2005**, *50*, 2597.

(20) Lakowitz, J. *Principles of Fluorescence Spectroscopy*, 2nd ed.; Springer: New York, 1999.

(21) Di Mascio, P.; Sies, H. *J. Am. Chem. Soc.* **1989**, *111*, 2909.

(22) Grossi, L.; Montevecchi, P. C. *J. Org. Chem.* **2002**, *67*, 8625.

(23) Oushiki, D.; Kojima, H.; Terai, T.; Arita, M.; Hanaoka, K.; Urano, Y.; Nagano, T. *J. Am. Chem. Soc.* **2010**, *132*, 2795.

(24) Snyder, J. W.; Skovsen, E.; Lambert, J. D. C.; Poulsen, L.; Ogilby, P. R. *Phys. Chem. Chem. Phys.* **2006**, *8*, 4280.

(25) Helmig, S. W.; Rotaru, A.; Arian, D.; Kovbasyuk, L.; Arnbjerg, J.; Ogilby, P. R.; Kjems, J.; Mokhir, A.; Besenbacher, F.; Gothelf, K. V. *ACS Nano* **2010**, *4*, 7475.

(26) Pattison, F. L. M.; Brown, G. M. *Can. J. Chem.* **1956**, *34*, 879.

(27) Diekers, M.; Luo, C.; Guldi, D.; Hirsch, A. *Chem.—Eur. J.* **2002**, *8*, 979.